Scientific Research Publishing

American Journal of Analytical Chemistry, 2020, 11, 172-186
https://www.scirp.org/journal/ajac
ISSN Online: 2156-8278
ISSN Print: 2156-8251

Analytical Solution of the Non-Linear Equation in Biodegradation of N-Butanol in a Biofilter

K. Saranya[1], V. Mohan[1], L. Rajendran[2*]

[1]Department of Mathematics, Thiagarajar College of Engineering, Madurai, India
[2]Department of Mathematics, AMET Deemed to be University, Chennai, India
Email: saranyak463@gmail.com, mohanvtce@gmail.com, *raj_sms@rediffmail.com

How to cite this paper: Saranya, K., Mohan, V. and Rajendran, L. (2020) Analytical Solution of the Non-Linear Equation in Biodegradation of N-Butanol in a Biofilter. *American Journal of Analytical Chemistry*, **11**, 172-186.
https://doi.org/10.4236/ajac.2020.114013

Received: March 1, 2020
Accepted: April 17, 2020
Published: April 20, 2020

Abstract

In this paper, mathematical models of biofilm mixtures of n-butanol biofilters were discussed. The model is based on the mass transfer in the biofilm interface and chemical oxidation in the biofilm phase and gas phase. An approximate analytical expression of concentration profiles of n-butanol in the biofilm phase and gas phase has been derived using the homotopy perturbation method and hyperbolic function method for all possible values of parameters. Furthermore, in this work, the numerical simulation of the problem is also reported using the Matlab program. Good agreement between the analytical and numerical results is noted. Graphical results are presented and discussed quantitatively to illustrate the solution. The analytical results will be useful in finding the yields of biomass and oxygen consumption, the specific biomass surface area, activation energy and saturation constant for the Michaelis-Menten kinetics.

Keywords

Mathematical Modeling, Nonlinear Differential Equations, Biofilters, Biodegradation, Diffusion Limitation, Kinetics

1. Introduction

Several volatile organic compounds such as n-butanol, acetone, styrene, toluene, and DMDS are emanated from industrial sources that are unhealthy to humanistic well-being and may motive vomiting, irritability and upset the nervous and respiratory systems [1]. VOCs imperil air aspect and inartificial environs by giving greenhouse consequences and cooperate in the generation of the stratospheric ozone layer [1]. Also, Ketones Lee *et al.* [2] successfully applied the biofiltration technology for the deterioration of some hydrophilic compounds such as

liquors and, oxygen must also disband in the damp layer and spread to the biofilm [3]. In a macro kinetic approach, it is assumed that mass relocates restraint can be ignored [4] [5]. A few results have shown that macro kinetics models fit well with the experimental elimination capacities (EC's) [6] [7] [8] [9], though there are several models and expressions available in the literature that corresponds to various phenomena and processes at biofilter. Eshraghi *et al.* [10] studied the effect of operating temperature on the removal of n-butanol vapor in a biofilter.

To the best of our knowledge, there is no rigorous analytical expression available to date for the steady-state concentration. As a result, in this work, we focus on obtaining a feeling for the steady-state concentration of n-butanol in the biofilm phase and gas phase. Further, the expression helps us to analyze the physical response related to the parameters in the biofilter model.

2. Mathematical Modeling of the Boundary Value Problem

The modeling was developed by using the following assumption [10]:

- The biofilm is formed on the outside surface of the packing materials, and there is no reaction in the pores and the biofilm completely covers the surface of the packaging materials.
- Compared to the size of solid particles, the biofilm is very thin; hence planar geometry is used.
- n-butanol is the sole reactant that influences the biodegradation rate, and oxygen does not limit the reaction.
- Arrhenius equation is used for the temperature dependence of the biodegradation rate constant.
- The plug flow model is applied to the gas phase.
- The air/biofilm interface concentration of n-butanol meets Henry's rule by assuming the same air/water partition coefficients.
- There is no boundary layer at the air/biofilm interface. Thus, gas-phase resistance is assumed negligible.
- The biofilm properties (δ, A_s and density) are constant all over the bed.
- The temperature gradient inside the biofilm is negligible.

1) Mass Balance in the Biofilm Phase

The steady-state mass balance equation for Michaelis-Menten kinetics in the biofilm may be written as follows [11]:

$$D\frac{\mathrm{d}^2 S}{\mathrm{d}x^2} = \mathrm{e}^{\frac{-E}{R}\left(\frac{1}{T}-\frac{1}{T_{ref}}\right)}\frac{EC_{\max}S}{K_m + S} \tag{1}$$

where S is the concentration of n-butanol, $EC_{\max}$ is the maximum of elimination capacity K_m is the Michaelis-Menten constant, D is the diffusion coefficient, E is the activation energy, R is the ideal gas constant and T is the kelvin temperature. The boundary conditions Eshraghi *et al.* [10] for the above equation at the air/biofilm interface are as follows:

$$\text{At } x=0,\ \ S=\frac{C}{H} \tag{2}$$

$$\text{At } x=\delta,\ \ \frac{\mathrm{d}S}{\mathrm{d}x}=0 \tag{3}$$

2) Mass Balance in Gas Phase

The concentration profile of n-butanol in the gas phase may be written as follows:

$$u\frac{\mathrm{d}C}{\mathrm{d}z}=A_S D\left[\frac{\mathrm{d}S}{\mathrm{d}x}\right]_{x=0} \tag{4}$$

where u is the superficial velocity of gas flow, A_S is the biofilm specific area, C is the n-butanol concentration in the gas phase and D is diffusion coefficient. The corresponding boundary condition is

$$\text{At } z=0,\ \ C=C_i \tag{5}$$

3) Dimensionless Mass Balance Equation in the Biofilm Phase

The non-linear differential Equation (1) is made dimensionless form by defining the following dimensionless parameters:

$$S^*=\frac{S}{S_i},\ x^*=\frac{x}{\delta},\ \phi=\frac{\delta^2 \mathrm{e}^{-\frac{E}{R}\left(\frac{1}{T}-\frac{1}{T_{ref}}\right)}EC_{\max}}{DK_m},\ \beta=\frac{S_i}{K_m} \tag{6}$$

Using the above dimensionless variables, Equation (1) reduces to the following dimensionless form:

$$\frac{\mathrm{d}^2S^*}{\mathrm{d}x^{*2}}=\phi\left(\frac{S^*}{1+\beta S^*}\right) \tag{7}$$

The corresponding boundary conditions for the above Equation (7) can be expressed as

$$S^*=1 \quad \text{at } x^*=0 \tag{8}$$

$$\frac{\mathrm{d}S^*}{\mathrm{d}x^*}=0 \ \text{ at } x^*=1 \tag{9}$$

4) Dimensionless Mass Balance in the Gas Phase

By defining the following dimensionless parameters, the differential Equation (4) is made dimensionless form:

$$C^*=\frac{C}{C_i},\ \ z^*=\frac{z}{H},\ \ x^*=\frac{x}{\delta},\ \ A=\frac{HA_S DS_i}{u\delta C_i} \tag{10}$$

Using the variables, Equation (4) can be expressed in the dimensionless form as follows:

$$\left(\frac{\mathrm{d}C^*}{\mathrm{d}z^*}\right)=A\left(\frac{\mathrm{d}S^*}{\mathrm{d}x^*}\right)_{x^*=0} \tag{11}$$

The respective boundary condition for the above mentioned Equation (11) can be described as

$$C^*=1 \quad \text{at } z^*=0 \tag{12}$$

3. Analytical Expression for the Concentrations for Values of Parameter Using HPM

HPM couples the homotopy technology and perturbation. The primary deficiencies in applying perturbation methods are that a small parameter is needed in the equations. The HPM was further developed and improved and applied to nonlinear oscillators [11], nonlinear wave equations [12], boundary value problem [13], bifurcation problems [14], etc. Abukhaled and Khuri [15] obtained a semi-analytical solution of nonlinear equations in amperometric enzymatic reactions. This method was based on constructing a Green's function and employing a fixed point iterative scheme [16] [17]. In recent years, the application of the homotopy perturbation method in nonlinear problems has been developed by scientists and engineers [18] [19]. Most perturbation methods assume a small parameter exists, but most nonlinear problems have no small parameter at all. Unlike analytical perturbation methods, the HPM and HAM do not depend on a small parameter, which is difficult to find [20] [21]. Using the homotopy perturbation method (**Appendix A**), the concentration of n-butanol in the biofilm phase is obtained as follows:

$$S^*\left(x^*\right)=\frac{\cosh\sqrt{\phi}\left(x^*-1\right)}{\cosh\sqrt{\phi}}-\frac{\beta\cosh 2\sqrt{\phi}\left(x^*-1\right)}{6\cosh^2\sqrt{\phi}}+\frac{\beta}{2\cosh^2\sqrt{\phi}}+\left[\frac{\beta\cosh 2\sqrt{\phi}}{6\cosh^2\sqrt{\phi}}-\frac{\beta}{2\cosh^2\sqrt{\phi}}\right]\left[\frac{\cosh\sqrt{\phi}\left(x^*-1\right)}{\cosh\sqrt{\phi}}\right] \tag{13}$$

Solving Equation (11) using boundary condition (12) the concentrations of n-butanol in gas phase can be obtained as follows:

$$C^*\left(z^*\right)=1+z^*A\tanh\sqrt{\phi}\left[\frac{2\beta\sqrt{\phi}}{3}-1-\sqrt{\phi}\left(\frac{\beta\cosh 2\sqrt{\phi}}{6\cosh^2\sqrt{\phi}}-\frac{\beta}{2\cosh^2\sqrt{\phi}}\right)\right] \tag{14}$$

4. Analytical S Expression for the Concentrations Using Hyperbolic Function Method

In order to use the new analytical method, the trail solution for Equation (7) is given below:

$$S^*\left(x^*\right)=A\cosh\left(mx^*\right)+B\sinh\left(mx^*\right) \tag{15}$$

where A, B, m are constants. Using the boundary conditions (8) and (9), we get the constant

$$A=1,\quad B=-\frac{\sinh\left(m\right)}{\cosh\left(m\right)} \tag{16}$$

Now Equation (15) reduces to

$$S^*\left(x^*\right)=\cosh\left(mx^*\right)-\frac{\sinh\left(m\right)}{\cosh\left(m\right)}\sinh\left(mx^*\right) \tag{17}$$

where m is constant. This constant can be obtained as follows:

Equation (7) can be rewritten as

$$\frac{\mathrm{d}^2 S^*\left(x^*\right)}{\mathrm{d}x^{*2}} = m^2 \cosh\left(mx^*\right) - \left(\frac{\sinh(m)}{\cosh(m)}\right) m^2 \sinh\left(mx^*\right) \tag{18}$$

Substituting Equation (18) in Equation (7), we get the following result.

$$\begin{aligned} & m^2 \cosh\left(mx^*\right) - \left(\frac{\sinh(m)}{\cosh(m)}\right) m^2 \sinh\left(mx^*\right) \\ & = \frac{\phi\left(\cosh\left(mx^*\right) - \left(\frac{\sinh(m)}{\cosh(m)}\right)\sinh\left(mx^*\right)\right)}{1+\beta\left(\cosh\left(mx^*\right) - \left(\frac{\sinh(m)}{\cosh(m)}\right)\sinh\left(mx^*\right)\right)} \end{aligned} \tag{19}$$

When $x = 0$, the above results becomes

$$m^2 = \frac{\phi}{1+\beta} \tag{20}$$

Using Equation (20), the value of m becomes as follows:.

$$m = \sqrt{\frac{\phi}{1+\beta}} \tag{21}$$

The concentration of n-butanol can be obtained in the biofilm process by inserting Equation (21) in Equation (17), as follows:

$$\begin{aligned} S^*\left(x^*\right) &= \cosh\left(\sqrt{\frac{\phi}{1+\beta}}\, x\right) - \frac{\sinh\left(\sqrt{\frac{\phi}{1+\beta}}\right)}{\cosh\left(\sqrt{\frac{\phi}{1+\beta}}\right)} \sinh\left(\sqrt{\frac{\phi}{1+\beta}} x\right) \\ &= \frac{\cosh\left(\sqrt{\frac{\phi}{1+\beta}}\,(x-1)\right)}{\cosh\left(\sqrt{\frac{\phi}{1+\beta}}\right)} \end{aligned} \tag{22}$$

Hyperbolic function method is a special case of exponential function method [22].

5. Results and Discussion

Equations (13) & (14) represent the simple and new analytical expressions of the concentration of n-butanol in biofilm-phase (S^*) and in the gas-phase (C^*) respectively. The concentration of n-butanol in the biofilm-phase and the gas-phase depends upon the parameters ϕ and β. The variation in the dimensionless variable ϕ can be achieved by varying either the thickness (δ) or diffusivity of the biofilm (D). The parameter β depends upon the initial concentration (S_i) and half-saturation constant (K_m).

The experimental setup for the biofiltration of this organic compound is given in **Figure 1**. **Figure 2** represents the concentration of n-butanol S^* in the biofilm phase versus dimensionless height x^* for different values of β and ϕ. From **Figure 2(a)**, it is inferred that the concentration of n-butanol increases

when ϕ decreases for the fixed value of β. Figure 2(b), represents the concentration of n-butanol in the biofilm-phase increases when β increases for some fixed values of ϕ.

Figure 3 exhibits the concentration of n-butanol C^* in the gas phase for different values of A, ϕ and β. From Figure 3(a), it is inferred that the concentration of n-butanol in the gas phase increases when ϕ, A decreases From Figure 3(b), it is observed the concentration of n-butanol in the gas phase increases when β increases. From Figure 3(c), it is inferred that the concentration of n-butanol in the gas phase increases when A decreases for the fixed value of ϕ and β. Figure 4

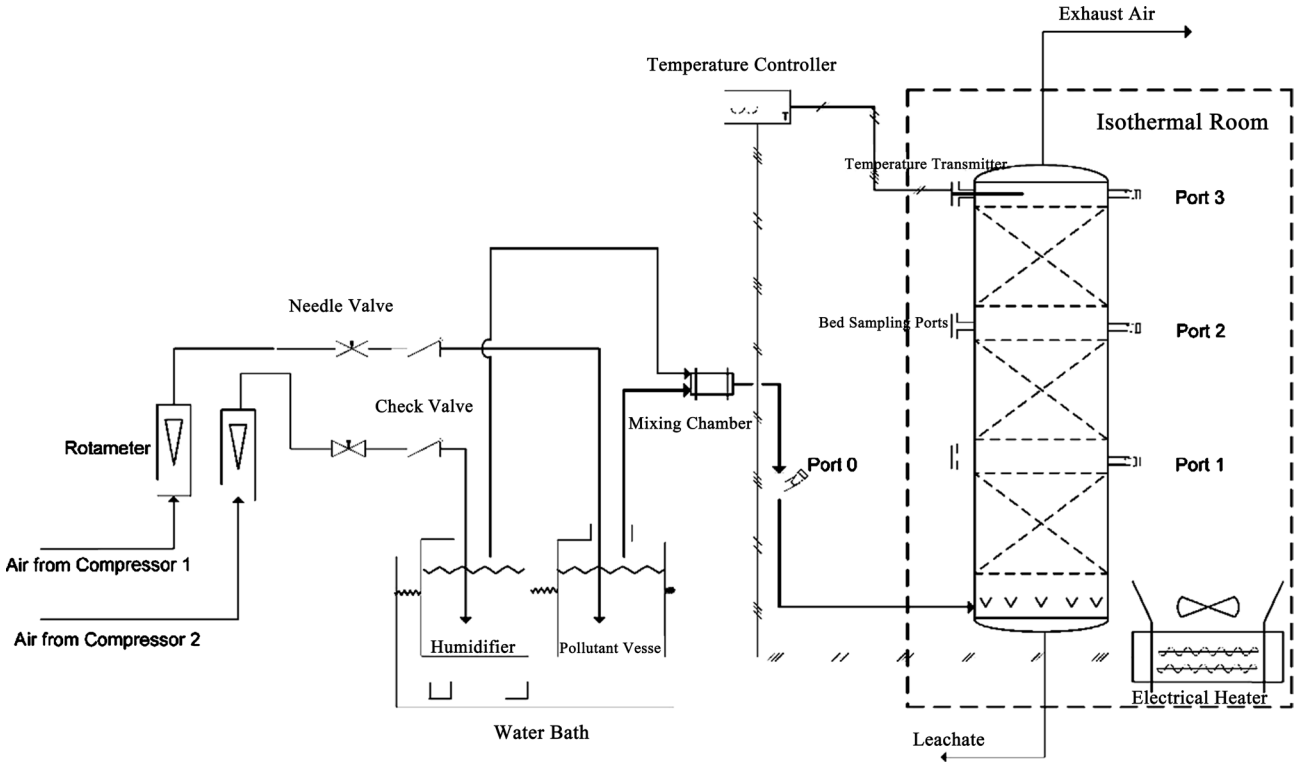

Figure 1. Schematic of the laboratory BF set up [10].

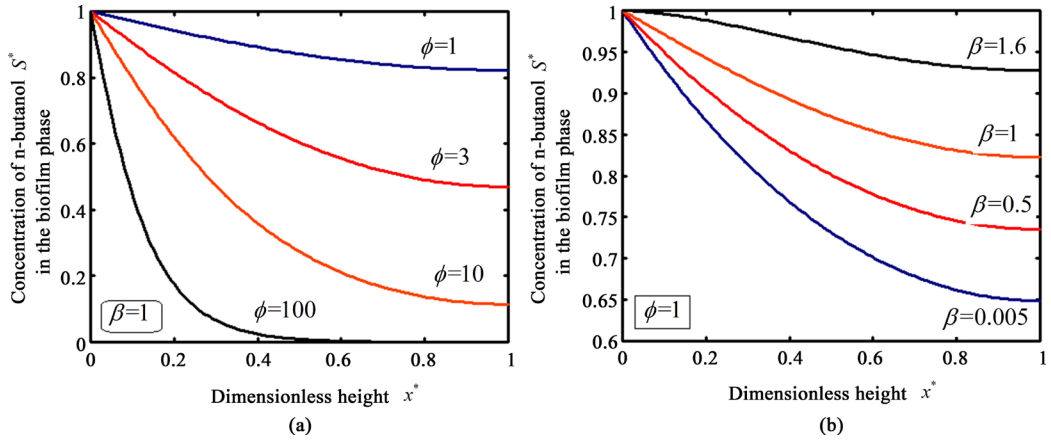

Figure 2. (a) Effect of parameter ϕ on the concentration of n-butanol S^* in the biofilm phase using Equation (13); (b) Effect of parameter β on the concentration of n-butanol S^* in the biofilm phase using Equation (13).

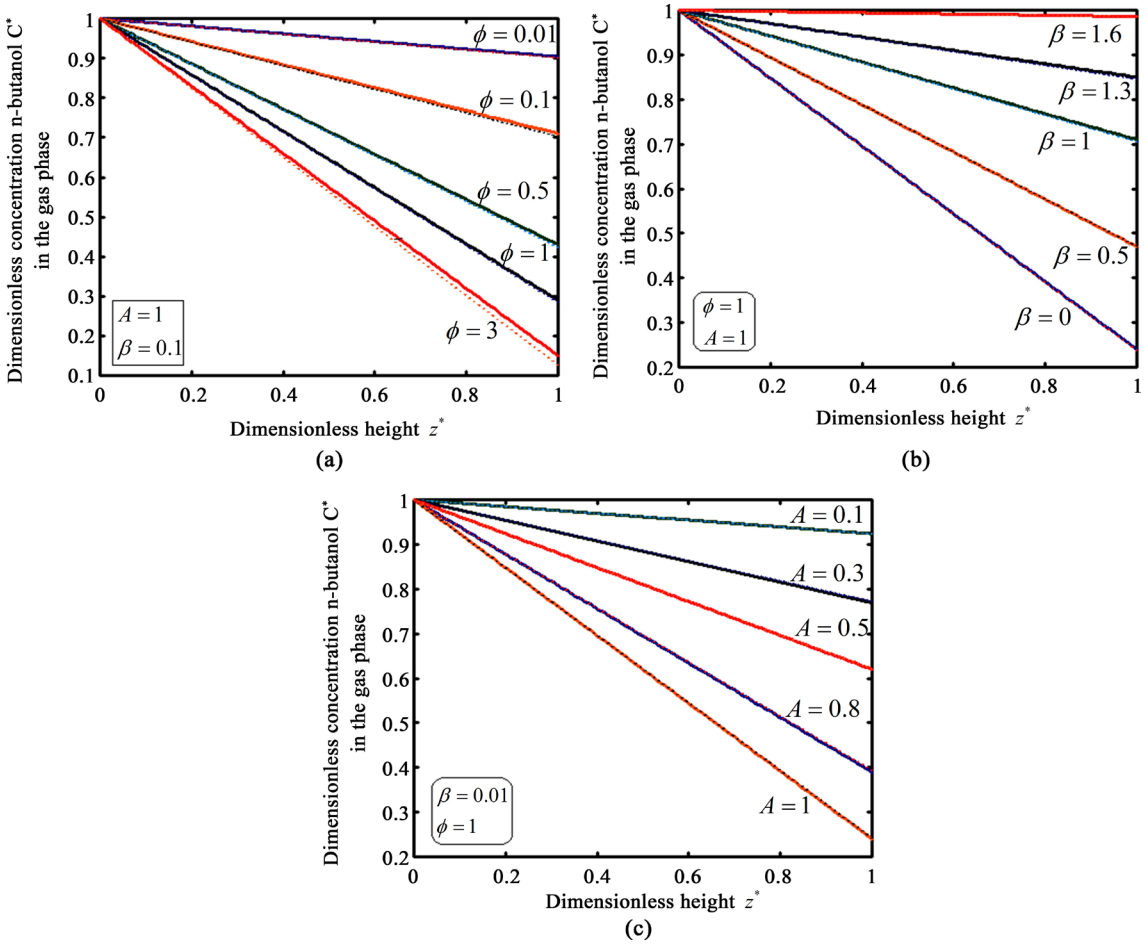

Figure 3. Comparison of concentration n-butanol C^* in the gas phase with simulation results, when (a) $\beta = 0.1$ for various values of the parameter ϕ; (b) $\phi = 1$ for various values of the parameter β and (c) $\phi = 1, \beta = 0.01$ for various values of the parameter A. The key to the graph: Solid lines represented the numerical simulation and dotted lines represent Equation (14).

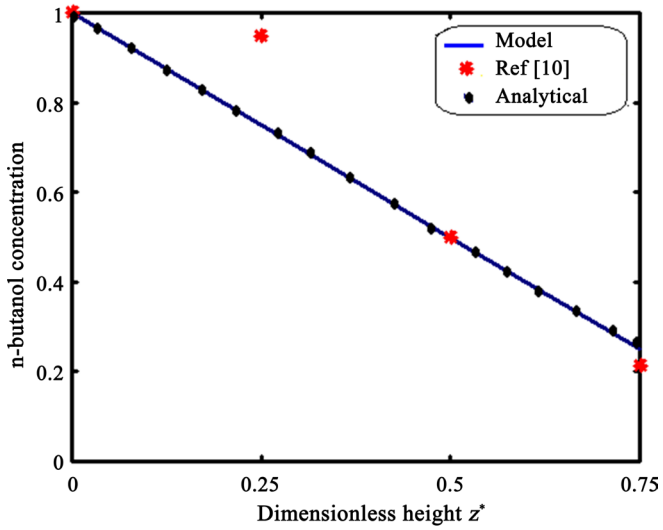

Figure 4. Comparison of concentration of n-butanol Equation (14) with experimental result [10] for the parameters $\phi = 10$ & $\beta = 0.0001$.

represents n-butanol concentration for different values of z^* and compared with analytical method numerical simulation and experimental results (Eshraghi *et al.* 2016).

6. Differential Sensitivity Analysis of Parameters

The sensitivity analysis of the parameter is given in Figure 5 & Figure 6. From the analysis it is inferred that the reaction and diffusion parameter ϕ, β have more impact in the concentration S^* in the biofilm-phase. In contrast, the parameter A has more impact in the concentration C^* in gas-phase.

7. Numerical Simulation

In order to investigate the accuracy of the HPM solution with a finite number of terms, the nonlinear differential equation is solved numerically. To show the efficiency of the present method, the analytical expressions of the concentration of n-butanol in biofilm-phase and gas-phase are compared with simulation results in Tables 1-3 for the experimental values of parameters. A satisfactory agreement is

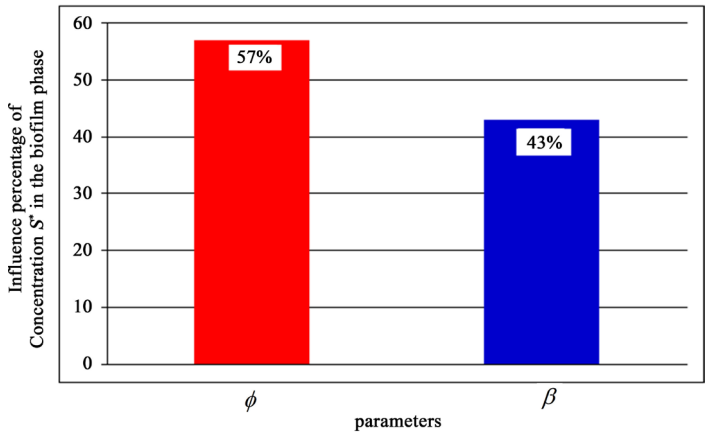

Figure 5. Sensitivity analysis of parameters on concentration of n-butanol in the biofilm-phase.

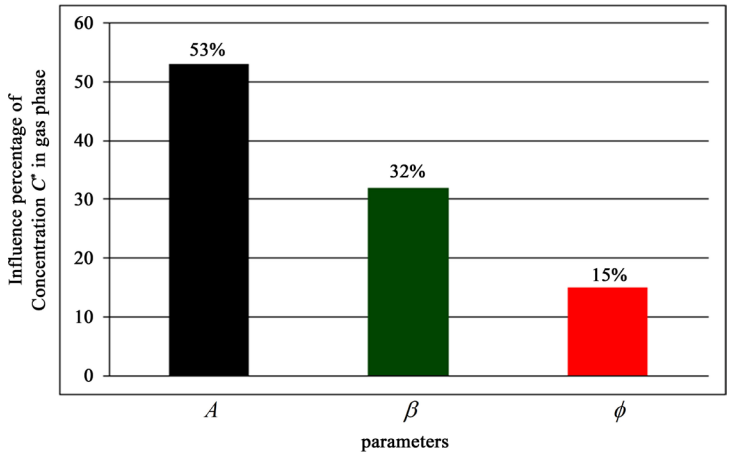

Figure 6. Sensitivity analysis of parameters on concentration of n-butanol in gas-phase.

Table 1. Comparison of normalized non-steady-state concentration S^* with simulation results when $\beta = 1$.

x^*	Concentration S^* when $\phi = 1$					when $\phi = 10$					when $\phi = 100$				
	Simulation	(HPM)Equation (13)	hyperbolic function method Equation (22)	% of error deviation (HPM) Equation (13)	% of error deviation hyperbolic function method Equation (22)	Simulation	(HPM) Equation (13)	hyperbolic function method Equation (22)	% of error deviation (HPM) Equation (13)	% of error deviation hyperbolic function method Equation (22)	Simulation	Equation (13)	hyperbolic function method Equation (22)	% of Error deviation (HPM) Equation (13)	% of error deviation hyperbolic function method Equation (22)
0	1.0000	1.0000	1.0000	0.00	0.00	1.0000	1.0000	1.0000	0.00	0.00	1.0000	1.0000	1.0000	0.00	0.00
0.2	0.8998	0.9425	0.9236	4.53	2.64	0.6117	0.6188	0.6498	1.14	5.86	0.1700	0.1743	0.1810	2.46	6.07
0.4	0.8486	0.8924	0.8657	4.90	2.01	0.3535	0.3598	0.3701	1.75	4.48	0.0235	0.0243	0.0249	3.40	5.62
0.6	0.8082	0.8543	0.8252	5.39	2.06	0.2069	0.2107	0.2196	1.83	5.78	0.0032	0.0033	0.0034	3.12	5.88
0.8	0.7898	0.8306	0.8012	5.15	1.42	0.1338	0.1367	0.1389	2.16	3.67	0.0004	0.0004	0.0004	0.00	0.00
1	0.7768	0.8226	0.7932	5.56	2.06	0.1121	0.1147	0.1189	2.26	5.71	0.0001	0.0001	0.0001	0.00	0.00
Average error %				4.25	1.69	Average error %			1.52	4.25	Average error %			1.49	2.92

Table 2. Comparison of normalized non-steady-state concentration C^* with simulation results when $\beta = 0.1$ and $A = 1$.

z^*	Concentration C^* when $\phi = 0.01$			when $\phi = 0.1$			when $\phi = 1$		
	Equation (14)	Simulation	% of Error deviation	Equation (14)	Simulation	% of error deviation	Equation (14)	Simulation	% of Error deviation
0	1.0000	1.0000	0.00	1.0000	1.0000	0.00	1.0000	1.0000	0.00
0.2	0.9801	0.9806	0.05	0.9400	0.9414	0.14	0.8556	0.8566	0.11
0.4	0.9601	0.9612	0.11	0.8800	0.8828	0.31	0.7112	0.7131	0.26
0.6	0.9402	0.9418	0.16	0.8200	0.8242	0.50	0.5667	0.5697	0.52
0.8	0.9203	0.9224	0.22	0.7600	0.7657	0.74	0.4223	0.4263	0.93
1	0.9013	0.9040	0.29	0.7030	0.7100	0.99	0.2851	0.2900	1.68
Average error % 0.138				Average error % 0.446			Average error % 0.583		

Table 3. Comparison of normalized non-steady-state concentration C^* with simulation results when $\phi = 1$ and $A = 1$.

z^*	Concentration C^* when $\beta = 0.5$			when $\beta = 1$			when $\beta = 1.6$		
	Equation (14)	Simulation	% of error deviation	Equation (14)	Simulation	% of error deviation	Equation (14)	Simulation	% of error deviation
0	1.0000	1.0000	0.00	1.0000	1.0000	0.00	1.0000	1.0000	0.00
0.2	0.8933	0.8929	0.04	0.9405	0.9411	0.06	0.9971	0.9971	0.00
0.4	0.7866	0.7859	0.08	0.8810	0.8822	0.13	0.9943	0.9942	0.01
0.6	0.6800	0.6788	0.17	0.8215	0.8233	0.21	0.9914	0.9914	0.00
0.8	0.5733	0.5717	0.27	0.7620	0.7644	0.31	0.9886	0.9885	0.01
1	0.472	0.4700	0.42	0.7055	0.7055	0.00	0.9857	0.9858	0.01
Average error % 0.163				Average error % 0.118			Average error % 0.005		

noted. The detailed Matlab program for numerical simulation is provided in **Appendix B** and **Appendix C**.

8. Conclusion

In this paper, the non-linear differential equations in the biofiltration have been solved analytically. Using the homotopy perturbation method and hyperbolic function method, an approximate and closed-form of analytical representation of the concentrations of n-butanol in the biofilm phase is provided. This solution of the concentrations of n-butanol in the biofilm phase and the gas phase is compared with the numerical simulation results. These new analytical results provide a good understanding of the system and the optimization of the parameters in the biofiltration model.

Acknowledgements

This work was supported by consultancy project, Academy of Maritime Education and Training (AMET), Deemed to be University, Chennai. The Authors are also thankful to Shri J. Ramachandran, Chancellor, Col. Dr. G. Thiruvasagam, Vice-Chancellor, Academy of Maritime Education and Training (AMET), Deemed to be University, Chennai, for their constant encouragement.

Conflicts of Interest

The authors declare no conflicts of interest regarding the publication of this paper.

References

[1] Munoz, R., Daugulis, A.J., Hernandez, M. and Quijano, G. (2012) Recent Advances in Two-Phase Partitioning Bioreactors for the Treatment of Volatile Organic Compounds. *Biotechnology Advances*, **30**, 1707-1720. https://doi.org/10.1016/j.biotechadv.2012.08.009

[2] Lee, C.L.S., Heber, A.J., Ni, J. and Huang, H. (2013) Biofiltration of a Mixture of Ethylene, Ammonia, N-Butanol, and Acetone Gases. *Bioresource. Technology*. **127**, 366-377. https://doi.org/10.1016/j.biortech.2012.09.110

[3] Devinny, J.S. and Ramesh, J. (2005) A Phenomenological Review of Biofilter Models. *Chemical Engineering Journal*, **113**, 187-196. https://doi.org/10.1016/j.cej.2005.03.005

[4] Delhomenie, M.C., Nikiema, J., Bibeau, L. and Heitz, M. (2008) A New Method to Determine the Microbial Kinetic Parameters in Biological Air Filters. *Chemical Engineering Science*, **63**, 4126-4134. https://doi.org/10.1016/j.ces.2008.05.020

[5] Ramirez, A.V., Benard, S., Giroir-Fendler, A., Jones, J.P. and Heitz, M. (2008) Kinetics of Microbial Growth and Biodegradation of Methanol and Toluene in Biofilters and an Analysis of the Energetic Indicators. *Journal of Biotechnology*, **138**, 88-95. https://doi.org/10.1016/j.jbiotec.2008.08.001

[6] Gebert, J., Groengroeft, A. and Miehlich, G. (2003) Kinetics of Microbial Landfill Methane Oxidation in Biofilters. *Waste Management*, **23**, 609-619. https://doi.org/10.1016/S0956-053X(03)00105-3

[7] Krailas, S. and Pham, Q.T. (2002) Macrokinetic Determination and Water Movement in a Downward Flow Biofilter for Methanol Removal. *Biochemical Engineering Journal*, **10**, 103-113. https://doi.org/10.1016/S1369-703X(01)00165-6

[8] Lim, K.H. (2001) Waste Air Treatment with a Biofilter: For the Case of Excess Adsorption Capacity. *Journal of Chemical Engineering of Japan*, **34**, 766-775. https://doi.org/10.1252/jcej.34.766

[9] Streese, J., Schlegelmilch, M., Heining, K. and Stegmann, R. (2005) A Macrokinetic Model for Dimensioning of Biofilters for VOC and Odour Treatment. *Waste Management*, **25**, 965-974. https://doi.org/10.1016/j.wasman.2005.07.009

[10] Eshraghi, M., Parnian, P., Zamir, S.M. and Halladj, R. (2016) Biofiltration of N-Butanol Vapour at Different Operating Temperatures: Experiment Study and Mathematical Modeling. *International Biodeterioration & Biodegradation*, **119**, 361-367. https://doi.org/10.1016/j.ibiod.2016.10.012

[11] He, J.H. (2004) The Homotopy Perturbation Method for Non-Linear Oscillators with Discontinuities. *Applied Mathematics and Computation*, **151**, 287-292. https://doi.org/10.1016/S0096-3003(03)00341-2

[12] He, J.H. (2005) Application of Homotopy Perturbation Method to Nonlinear Wave Equations. *Chaos Solitons Fractals*, **26**, 695-700. https://doi.org/10.1016/j.chaos.2005.03.006

[13] He, J.H. (2006) Homotopy Perturbation Method for Solving Boundary Problems. *Physics Letters A*, **350**, 87-88. https://doi.org/10.1016/j.physleta.2005.10.005

[14] He, J.H. (2005) Limit Cycle and Bifurcation of Nonlinear Problems. *Chaos Solitons Fractals*, **26**, 827-833. https://doi.org/10.1016/j.chaos.2005.03.007

[15] Abukhaled, M. and Khuri, S.A. (2017) A Semi-Analytical Solution of Amperometric Enzymatic Reactions Based on Green's Functions and Fixed Point Iterative Schemes. *Journal of Electroanalytical Chemistry*, **792**, 66-71. https://doi.org/10.1016/j.jelechem.2017.03.015

[16] Abukhaled, M. (2017) Green's Function Iterative Method for Solving a Class of Boundary Value Problems Arising in Heat Transfer. *Applied Mathematics & Information Sciences*, **11**, 229-234. https://doi.org/10.18576/amis/110128

[17] Abukhaled, M. (2017) Green's Function Iterative Approach for Solving Strongly Nonlinear Oscillators. *The Journal of Computational and Nonlinear Dynamics*, **12**, Article ID: 051021. https://doi.org/10.1115/1.4036813

[18] He, J.H. (2004) Asymptotology by Homotopy Perturbation Method. *Applied Mathematics and Computation*, **156**, 591-596. https://doi.org/10.1016/j.amc.2003.08.011

[19] He, J.H. (2005) Homotopy-Perturbation Method for Bifurcation of Nonlinear Problems. *International Journal of Nonlinear Science and Numerical Simulation*, **6**, 207-208. https://doi.org/10.1515/IJNSNS.2005.6.2.207

[20] Liao, S.J. (2004) On the Homotopy Analysis Method for Nonlinear Problems. *Applied Mathematics and Computation*, **147**, 499-513. https://doi.org/10.1016/S0096-3003(02)00790-7

[21] Liao, S.J. (2009) Notes on the Homotopy Analysis Method: Some Definition and Theorems. *Communications in Nonlinear Science and Numerical Simulation*, **14**, 983-997. https://doi.org/10.1016/j.cnsns.2008.04.013

[22] He, J.H. (2019) A Simple Approach to One-Dimensional Convection-Diffusion Equation and Its Fractional Modification for E Reaction Arising in Rotating Disk Electrodes. *Journal of Electroanalytical Chemistry*, **854**, Article ID: 113565. https://doi.org/10.1016/j.jelechem.2019.113565

Nomenclature

Symbols	Description	Units
A_S	Biofilm specific area per unit volume of the biofilters	$\mathbf{m^{-1}}$
E	Activation energy	$J{\cdot}mol^{-1}$
k_m	Michaelis-Menten constant	$g{\cdot}m^{-3}$
u	Superficial velocity of gas flow	$m{\cdot}s^{-1}$
z	Dimension along the height of the biofilters	m
D	Effective diffusivity of n-butanol in the biofilm phase and gas phase.	$m^2{\cdot}s^{-1}$
$S=\frac{C}{H}=S_i$	Initial concentration of butanol in the biofilm	$g{\cdot}m^{-3}$
R	Ideal gas constant	J/Kelvin mole
T	Kelvin temperature (initial)	˚C
T_{ref}	Kelvin temperature (final)	˚C
$EC_{\max}$	Maximum of elimination capacity	$g{\cdot}m^{-3}{\cdot}h^{-1}$
δ	Biofilm thickness	m
C	Concentration of n-butanol in the gas phase	$g{\cdot}m^{-3}$
C_i	Concentration of n-butanol in the inlet gas phase	$g{\cdot}m^{-3}$
H	Total height of the biofilters	m
$S^*=\frac{S}{S_i}$	Dimensionless concentration of n-butanol in the biofilm	none
$x^*=\frac{x}{\delta}$	Dimensionless height of the biofilm	none
$\phi=\frac{\delta^2 \mathrm{e}^{-\frac{E}{R}\left(\frac{1}{T}-\frac{1}{T_{ref}}\right)}EC_{\max}}{Dk_m}$	Thiele modulus	none
$\beta=\frac{S_i}{k_m}$	Characteristic length	none
$C^*=\frac{C}{C_i}$	Dimensionless concentration of n-butanol in the gas phase	none
$z^*=\frac{z}{H}$	Dimensionless height of the biofilters	none
$A=\frac{HA_SDS_i}{u\delta C_i}$	Dimensionless parameter	none

Supplementary Materials of the Manuscript

Appendix A: Analytical Solution of Equation (1) in Gas Phase Using HPM

The homotopy perturbation method is used to give the approximate solutions of the non-linear Equation (6). We construct the homotopy for Equation (1) as follows:

$$(1-p)\left(\frac{\mathrm{d}^2S^*}{\mathrm{d}x^{*2}}-\phi S^*\right)+p\left(\frac{\mathrm{d}^2S^*}{\mathrm{d}x^{*2}}+\beta S^*\frac{\mathrm{d}^2S^*}{\mathrm{d}x^{*2}}-\phi S^*\right)=0 \tag{A1}$$

The analytical solution of Equation (1) is

$$S^*=S_0^*+S_1^*p+S_2^*p^2+S_3^*p^3+\cdots \tag{A2}$$

Substituting Equation (A2) into Equation (A1) we get

$$\begin{aligned}&(1-p)\left[\frac{\mathrm{d}^2}{\mathrm{d}x^{*2}}\left(S_0^*+S_1^*p+S_2^*p^2+\cdots\right)-\phi\left(S_0^*+S_1^*p+S_2^*p^2\right)\right]\\&+p\left(\frac{\mathrm{d}^2}{\mathrm{d}x^{*2}}\left(S_0^*+S_1^*p+S_2^*p^2+\cdots\right)+\beta\left(S_0^*+S_1^*p+S_2^*p^2+\cdots\right)\right.\\&\left.\times\frac{\mathrm{d}^2}{\mathrm{d}x^{*2}}\left(S_0^*+S_1^*p+S_2^*p^2+\cdots\right)-\phi\left(S_0^*+S_1^*p+S_2^*p^2+\cdots\right)\right)=0\end{aligned} \tag{A3}$$

Comparing the coefficients of like powers of p in Equation (A3) we get

$$p^0:\left(\frac{\mathrm{d}^2S_0^*}{\mathrm{d}x^{*2}}-\phi S_0^*\right)=0 \tag{A4}$$

$$p^1:\left(\frac{\mathrm{d}^2S_1^*}{\mathrm{d}x^{*2}}-\phi S_1^*+\beta S_0^*\frac{\mathrm{d}^2S_0^*}{\mathrm{d}x^{*2}}\right)=0 \tag{A5}$$

The boundary conditions for Equation (A1) are as follows

$$S_0^*=1 \text{ at } x^*=0 \tag{A6}$$

$$\frac{\mathrm{d}S_0^*}{\mathrm{d}x^*}=0 \text{ at } x^*=1 \tag{A7}$$

Solving Equation (A4) and using the boundary conditions Equation (A6) and (A7), we obtain the following results:

$$S_0^*=C_1\cosh\sqrt{\phi}x^*+C_2\sinh\sqrt{\phi}x^* \tag{A8}$$

By applying the boundary conditions, we get C_1 and C_2

$$C_1=1,\quad C_2=-\frac{\sinh\sqrt{\phi}}{\cosh\sqrt{\phi}} \tag{A9}$$

Substitute C_1 & C_2 value in (A8) we get,

$$S_0^*\left(x^*\right)=\frac{\cosh\sqrt{\phi}\left(x^*-1\right)}{\cosh\sqrt{\phi}} \tag{A10}$$

Now Equation (A5) becomes

$$\frac{d^2 S_1^*}{\partial x^{*2}} - \phi S_1^* + \beta S_0^* \frac{d^2 S_0^*}{\partial x^{*2}} = 0 \quad \text{(A11)}$$

The boundary conditions for the above equation are as follows:

$$S_1^* = 0 \text{ at } x^* = 0 \quad \text{(A12)}$$

$$\frac{dS_1^*}{dx^*} = 0 \text{ at } x^* = 1 \quad \text{(A13)}$$

Solving Equation (A11) and using the boundary conditions Equations (A12) and (A13), we can get the following result:

$$S_1^*\left(x^*\right) = \frac{\beta}{2\cosh^2\sqrt{\phi}} - \frac{\beta}{6\cosh^2\sqrt{\phi}}\left[\cosh 2\sqrt{\phi}\left(x^* - 1\right)\right] + \left[\frac{\beta\cosh 2\sqrt{\phi}}{6\cosh^2\sqrt{\phi}} - \frac{\beta}{2\cosh^2\sqrt{\phi}}\right]\left[\frac{\cosh\sqrt{\phi}\left(x^* - 1\right)}{\cosh\sqrt{\phi}}\right] \quad \text{(A14)}$$

Considering the two terms, we get

$$s^*\left(x^*\right) = S_0^*\left(x^*\right) + S_1^*\left(x^*\right) \quad \text{(A15)}$$

which is Equation (15) in text.

Appendix B: Matlab Program for the Numerical Solution of Equation (1)

```
function pdex4
m = 0;
x = linspace(0,1);
t=linspace(0,1000000);
sol = pdepe(m,@pdex4pde,@pdex4ic,@pdex4bc,x,t);
u1 = sol(:,:,1);
%---------------------------------------------------------------
figure
plot(x,u1(end,:))
title('u1(x,t)')
xlabel('Distance x')
ylabel('u1(x,1)')
%---------------------------------------------------------------
function [c,f,s] = pdex4pde(x,t,u,DuDx)
c = 1;
f = 1.*DuDx;
k=5; B=0.005;
F1=-((k*u(1))/(1+(B*u(1))));
s=F1;
% ---------------------------------------------------------------
function u0 = pdex4ic(x)
u0 = [0];
% ---------------------------------------------------------------
```

```
function [pl,ql,pr,qr]=pdex4bc(xl,ul,xr,ur,t)
pl = [ul(1)-1];
ql = [0];
pr = [ur(1)-0];
qr = [1];
```

Appendix C: Matlab Program for the Numerical Solution of Equation (10)

```
function mat1
options=odeset('RelTol',1e-6,'stats','on');
%initial conditions
Xo=1;
tspan=[0 1];
tic
[t,X]=ode45(@TestFunction,tspan,Xo,options);
toc
figure
holdon
plot(t,X(:,1),'-');
t=0;
%plot(n,(100-100*X(:,1)),'-');
lgend('x1')
ylable('x')
xlable('t')
return
function [dx_dt]=Test Function(t,x)
A=0.8;m=1;B=0.01;
dx_dt(1)=A*((-tanh(sqrt(m)))+((B*sech(sqrt(m))*sech(sqrt(m))*sqrt(m)*(sinh(
2*(sqrt(m)))))/3))+(((B*sech(sqrt(m))*sech(sqrt(m))*cosh(2*(sqrt(m))))/6)-((B*
sech(sqrt(m))*sech(sqrt(m)))/2))*(-tanh(sqrt(m)));
return
```